

Tomisław Gołębiowski

 <https://orcid.org/0000-0002-4005-2265>

THEORETICAL ANALYSIS AND PRACTICAL VERIFICATION OF THE WORP TECHNIQUE APPLIED FOR THE GPR INVESTIGATION OF A FLOOD LEVEE

Krakow University of Technology, Faculty of Environmental Engineering and Energy,
Krakow, Poland

Abstract

The ground-penetrating radar (GPR) method is one of the geophysical electromagnetic methods. The standard technique of the GPR surveys is the short-offset reflection profiling (SORP) technique, which can theoretically be described in the same way as the zero-offset (ZO) measurements. During the surveys performed using the SORP technique, the offset (i.e. the separation between the transmitter and receiver antennae) is not adjusted to the depth of the objects located in an examined medium. In more advanced measurements, performed using the wide-offset reflection profiling (WORP) technique, the offset is adjusted to the supposed depth of the underground objects which should be detected using the GPR method. The theoretical background and comparison of the SORP and the WORP surveys were described in the paper. The article also presents theoretical analyses regarding to the shape of the radiation pattern generated by the GPR antennas located on the ground surface, i.e. on the border of two media (i.e. air and geological medium) with different electromagnetic properties. The variability of shapes of the radiation patterns as well as the variability of the reflection coefficients for electromagnetic waves with transverse electric (TE) and transverse magnetic (TM) polarizations for different offsets, affect the quality of GPR recordings, which was analysed in the paper theoretically as well as through the field tests. The terrain measurements were performed on a selected part of the Vistula river flood levee in Krakow (Poland), where geotechnical sounding indicated the existence of the loose zones. In order to increase the detection possibilities of the GPR method, surveys were performed after precipitation, which created a temporary two-layer medium, i.e. near-surface, water-saturated zone and deeper located, dry zone. The results of the WORP surveys confirmed the theoretical analysis and allowed to record more readable radargrams for larger offsets than in the case of the short offset, which facilitated further interpretation of the recordings.

Keywords: GPR, wide-offset surveys, flood levee

ANALIZA TEORETYCZNA I PRAKTYCZNA WERYFIKACJA ZASTOSOWANIA TECHNIKI WORP DO BADANIA WAŁU PRZECIWPOWODZIOWEGO METODĄ GPR

Abstrakt

Metoda georadarowa (ang. GPR – ground-penetrating radar) jest jedną z geofizycznych metod elektromagnetycznych. Standardową na dzień dzisiejszy techniką badań GPR jest krótko-offsetowe profilowanie refleksyjne (ang. SORP – short-offset reflection profiling), które teoretycznie można opisać identycznie jak pomiary zero-offsetowe (ZO). W badaniach wykonywanych techniką SORP nie dostosowuje się offsetu (tj. odległości między anteną nadawczą i odbiorczą) do głębokości położenia obiektów znajdujących się w rejonie badań. W bardziej zaawansowanych pomiarach wykonywanych techniką szeroko-offsetowego profilowania refleksyjnego (ang. WORP – wide-offset reflection profiling), offset dostosowany jest od domniemanej głębokości położenia obiektów podziemnych, które planujemy wykryć przy pomocy metody GPR. Założenia teoretyczne oraz porównanie pomiarów techniką SORP i WORP opisano w artykule. W artykule przedstawiono również analizy teoretyczne dotyczące kształtu pola radiacji fali dla anten GPR usytuowanych na powierzchni ziemi, tzn. na granicy dwóch ośrodków (tj. powietrze i ośrodek geologiczny) różniących się parametrami elektromagnetycznymi. Zmienność kształtu pola radiacji, jak również zmienność współczynników odbicia dla fal elektromagnetycznych o poprzecznej polaryzacji składowej elektrycznej

(ang. TE – transverse electric) i magnetycznej (ang. TM – transverse magnetic) przy różnych offsetach, wpływają na jakość rejestracji GPR, co przeanalizowano w artykule teoretycznie, jak również poprzez testy terenowe. Terenowe badania testowe wykonano na wybranym fragmencie wału przeciwpowodziowego rzeki Wisły w Krakowie (Polska), gdzie sondowania geotechniczne wskazywały na istnienie stref rozluźnień. W celu zwiększenia zdolności detekcyjnych metody GPR, pomiary wykonano po opadach, które stworzyły tymczasowy układ dwuwarstwowy, tzn. przypowierzchniowa strefa nasycona wodą oraz głębiej leżąca strefa sucha. Wyniki testowych badań techniką WORP potwierdziły założenia analizy teoretycznej i pozwoliły zarejestrować bardziej czytelne radargramy dla większych offsetów niż w przypadku krótkiego offsetu, co ułatwiło dalszą interpretację rejestracji.

Słowa kluczowe: metoda georadarowa, badania szeroko-offsetowe, wał przeciwpowodziowy

1. INTRODUCTION

The paper is a development of the presentation shown during the scientific conference [1], where the application of the ground-penetrating radar (GPR) method for examination of a flood levee was presented; only standard GPR measurement technique, i.e. the short-offset reflection profiling (SORP) technique, was presented during the conference. In the paper, the application of other GPR technique, i.e. the wide-offset reflection profiling (WORP) technique, applied for the same purpose, was shown. Basic information concerning the WORP may be found in the publication [2]; in the paper, more detailed theoretical aspects and data analysis in comparison with the publication [2] was presented.

The GPR method is one of geophysical, electromagnetic methods. Different measurement techniques are

implemented in this method, depending on the problems which should be solved; the following techniques may be distinguished:

- the short-offset reflection profiling (SORP), which may be treated as the zero-offset (ZO) technique,
- the wide-offset reflection profiling (WORP),
- velocity measurements, i.e. the common mid point (CMP) and the wide angle reflection refraction (WARR) techniques as well as analysis of the direct air wave (DAW),
- refraction surveys,
- transillumination of over-ground objects as well as borehole-borehole and borehole-surface tomography,
- surveys with application of different antennae orientations and different electromagnetic wave polarisations.



Fig. 1. Examples of typical configurations of the GPR systems produced by different geophysical companies – systems with: A) monostatic antenna (www.radsys.lv); B) nonseparated bistatic antennae (www.geophysical.com); C) separated shielded antennae (www.sensoft.ca); D) separated unshielded antennae (www.guidelinegeo.com)

Ryc. 1. Przykłady typowych systemów georadarowych produkowanych przez różne firmy geofizyczne – systemy z: A) anteną monostatyczną (www.radsys.lv); B) nierozseparowanymi antenami bistatycznymi (www.geophysical.com); C) rozseparowanymi antenami ekranowanymi (www.sensoft.ca); D) rozseparowanymi antenami nieekranowanymi (www.guidelinegeo.com)

Comparison of two first measurement techniques. i.e. the SORP and the WORP and discussion of the results obtained from both of them, were presented in the paper.

In the market, 3 constructions of the GPR systems are available, i.e.:

- systems with monostatic antenna (Fig. 1A),
- systems with bistatic antennae hosted in one shielded box (Fig. 1B),
- systems with separated, bistatic, shielded (Fig. 1C) and unshielded antennae (Fig. 1D).

For the WORP surveys, only systems presented in Fig. 1C, D may be used. For examination of a flood levee, special system was constructed (Fig. 2) which allowed to carry out simultaneously the SORP and the WORP surveys with the use of both, shielded and unshielded antennae. Two-channel control unit delivered by the MALA firm (www.guidelinegeo.com), named ProEx, was used for data acquisition. In the system presented in Fig. 2, unshielded antennae can be separated at any distances in range from 0.5 m (Fig. 2A) to

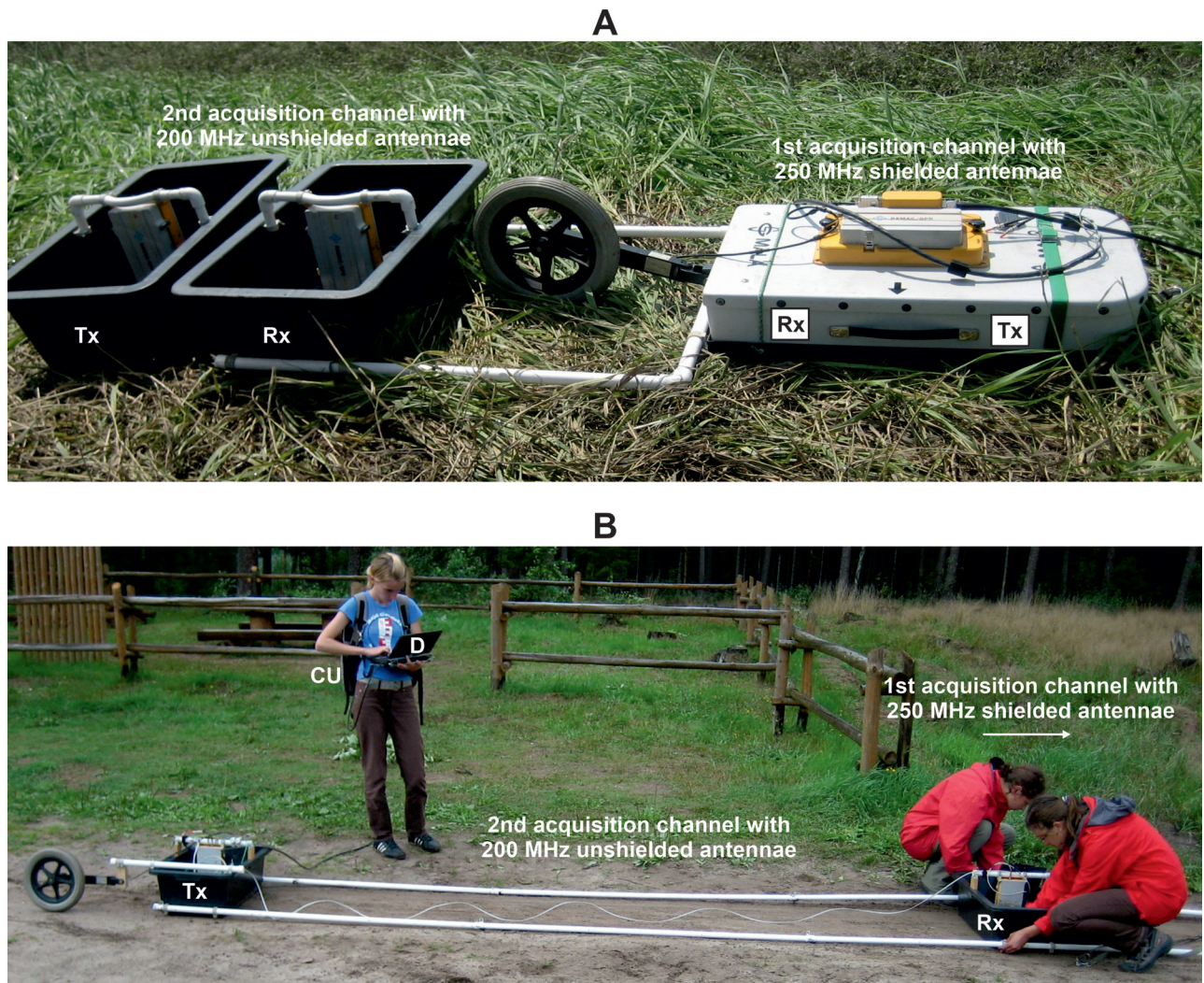


Fig. 2. 2-channel GPR system for simultaneous the SORP and the WORP surveys [2]: A) system configured for the SORP measurements in both channels; A) system configured for the SORP measurements in 1st channel and the WORP measurements in 2nd channel

Ryc. 2. Dwukanałowy system georadarowy do jednoczesnych badań krótko i szeroko-offsetowych [2]: A) system skonfigurowany do badań krótko-offsetowych na obu kanałach; B) system skonfigurowany do badań krótko-offsetowych na pierwszym kanale oraz szeroko-offsetowych na drugim kanale

5.0 m (Fig. 2B). Also two shielded antennae with the same frequency may be used for the WORP surveys and than measurements are realised as a cross-channel acquisition.

The terrain surveys on a flood levee were carried out with the use of shielded and unshielded antennae [Fig. 2] delivered by MALA firm, and the following configurations were applied:

- first acquisition channel – shielded 250 MHz antennae; second acquisition channel – unshielded 200 MHz antennae (these results are presented in the paper) and
- first acquisition channel – shielded 500 MHz antennae; second acquisition channel – unshielded 400 MHz antennae.

2. FUNDAMENTS OF THE GPR REFLECTION SURVEYS

Both the SORP and the WORP terrain surveys are conducted with the same way, i.e. the transmitter (Tx) and receiver (Rx) antennae are moving along profile with constant separation/offset S [m] between them. The Tx emits into the examined medium electromagnetic wave (i.e. transmitted wave – TW) which theoretically is described as a transvers electromagnetic (TEM) wave (Fig. 3A). The TW composes of electric (E) and magnetic (M) components and its propagation depends

on electromagnetic properties of the examined medium, i.e. ϵ_r [-] relative dielectric constant, μ_r [-] relative magnetic permeability and σ [mS/m] electrical conductivity. The GPR measurements presented in the paper were conducted in non-magnetic ground, so value of μ_r was assumed as 1 (Table 1) and was omitted in further analysis. The increase of electrical conductivity influences the increase of attenuation α [dB/m] of electromagnetic wave; the terrain surveys were carried out in the mixture of sand and silt (92%) with small amount of clay (8%), so attenuation in such medium should be relatively low (Table 1) and it did not play an important role during the terrain surveys. The Rx records along the profile the reflected waves (RW), at a specified and constant distance Δx (Fig. 3B). The recording is composed of several traces gathered every Δx and it is called radargram, which is presented in distance-time (x - t) plane. The vertical time axis t [ns] is converted into a depth axis z [m] on the basis of known velocity v [m/ns] of electromagnetic wave in the examined medium.

During the SORP surveys only 4 kinds of electromagnetic waves can be distinguished (Fig. 3B), i.e. the direct air wave (DAW), the direct ground wave (DGW), reflected wave (RW) and transmitted/incident wave (TW/IW). To simplify the theoretical analysis, it is often assumed for the SOPR technique that the geometry of ray paths is the same like for the zero-offset technique (Fig. 3C) and then the reflection coefficient R [-] can be expressed as [3]:

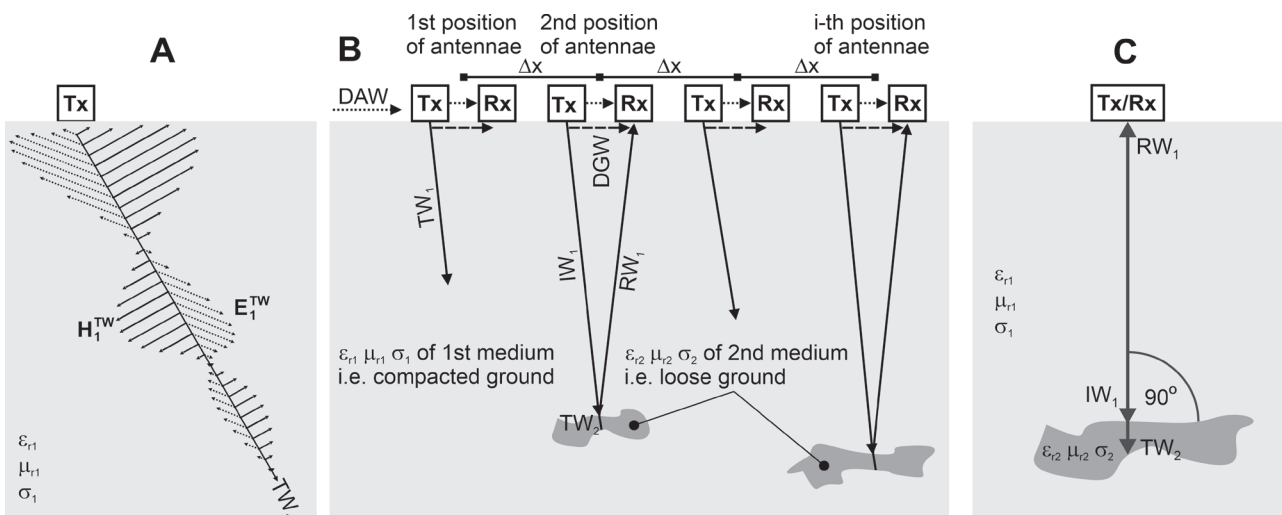


Fig. 3. A) Theoretical presentation of the TEM wave; B) Idea of the SORP surveys; C) Idea of the zero-offset ZO surveys

Ryc. 3. A) Teoretyczne przedstawienie fali elektromagnetycznej TEM; B) Idea pomiarów techniką SORP; C) Idea pomiarów techniką zero-offsetową ZO

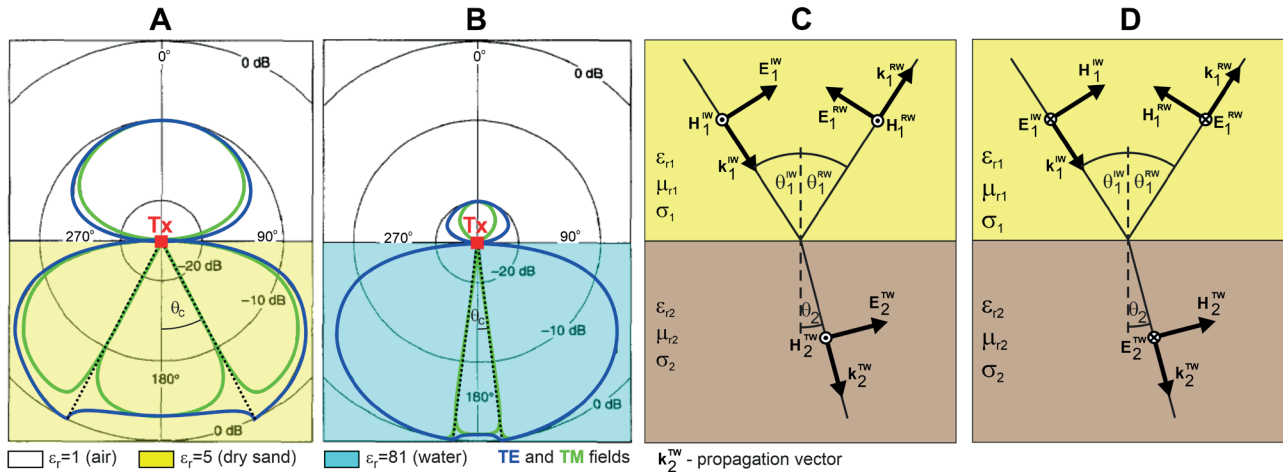


Fig. 4. Transverse magnetic TM and transverse electric TE components of the TEM wave, generated by the dipole Tx placed on the earth surface, counted for exemplary media, i.e., dry sand (A) and water (B) [5 – modified]; Reflections for different polarisation of the TEM wave, i.e., TM polarisation (C) and TE polarisation (D) [6]

Ryc. 4. Składowe TM i TE dla fali elektromagnetycznej typu TEM, wygenerowanej przez antenę dipolową leżącą na powierzchni ziemi, dla przykładowych ośrodków, tj. suchy piasek (A) i woda (B) [5 – zmodyfikowano]; Odbicia przy różnej polaryzacji fali elektromagnetycznej typu TEM, tzn. polaryzacja TM (C) i polaryzacja TE (D) [6]

$$R = \frac{\sqrt{\varepsilon_{r1}} - \sqrt{\varepsilon_{r2}}}{\sqrt{\varepsilon_{r1}} + \sqrt{\varepsilon_{r2}}} \quad (1)$$

where: ε_{r1} and ε_{r2} – relative dielectric constants of the 1st and the 2nd examined medium (Fig. 3).

In the publications [3, 4] was explained, that a practical reason for increasing antennae separation S is receiver dynamic range. The direct signals, i.e. the DAW and DGW (Fig. 3B), can be very large if the antennae separation is small. While electronic circuits may handle the overload safely, there is distortion and recovery time which make detection of shallow events impossible – this effect is called “transmit pulse blanking”. As minimum, value of S greater than half-wavelength ($\lambda/2$) generated by Tx is recommended. Depth resolution decreases as antennae separation increases, although this factor is small until separation approaches the target depth. The GPR antennas should be spaced such that the refraction focussing peak in Tx, defined by the critical angle θ_c [deg] (Fig. 4A, B) point to the common depth z [m] to be investigated; taking into account this assumption, the optimum antennae separation S is given by the expression [4]:

$$S = \frac{2z}{\sqrt{\varepsilon_{r1} - 1}} \quad (2)$$

During the WOPR surveys different kinds of electromagnetic waves can be distinguished (Fig. 5), i.e., the DAW, the DGW, the RW, the TW/IW and waves which are not recorded during the SORP measurements, i.e., the air-refracted wave (ARW) as well as the ground-refracted wave (GRW). The simplifications assumed for analysis of the ZO and the SORP surveys should not be taken into account now. For the WOPR measurements, the polarisations of the TEM wave during reflection should be analysed (Fig. 4C, D). For the WOPR technique, the reflection coefficients R_{TE} [-] and R_{TM} [-] are different, depending on situations presented in Fig. 4C, D, and can be expressed by the equations [4]:

$$R_{TM} = \frac{Z_1 \cdot \cos \theta_1 - Z_2 \cdot \cos \theta_2}{Z_1 \cdot \cos \theta_1 + Z_2 \cdot \cos \theta_2} \quad (3)$$

$$R_{TE} = \frac{Y_1 \cdot \cos \theta_1 - Y_2 \cdot \cos \theta_2}{Y_1 \cdot \cos \theta_1 + Y_2 \cdot \cos \theta_2} \quad (4)$$

$$Z = \frac{\sqrt{\mu_r \cdot \mu_0}}{\sqrt{\varepsilon_r \cdot \varepsilon_0}} \quad Y = \frac{1}{Z} \quad (5, 6)$$

where: Z [Ω] and Y [$1/\Omega$] – respectively the electromagnetic impedance and admittance; μ_0 [H/m] and ε_0 [F/m] – respectively magnetic permittivity and dielectric constant of vacuum.

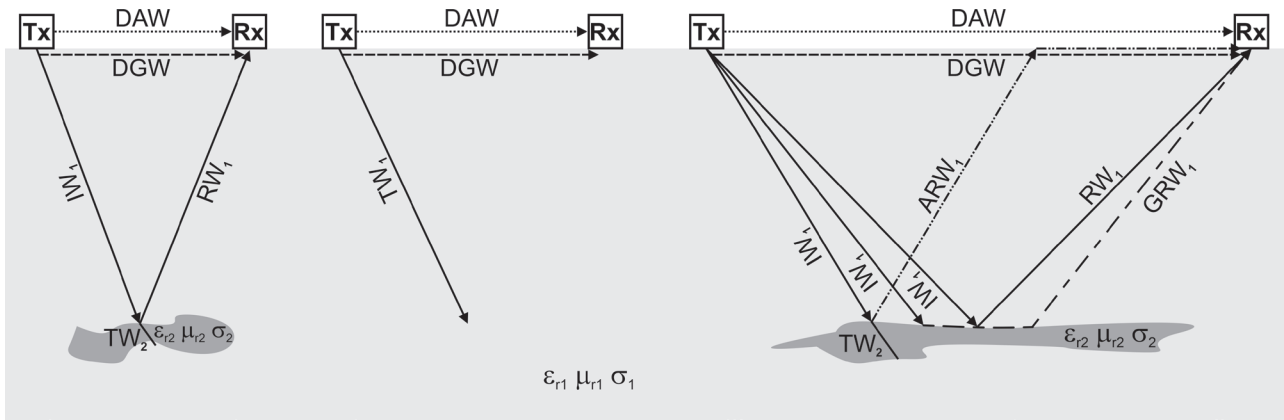


Fig. 5. Different kinds of electromagnetic waves recorded during the WORP surveys depending of offsets

Ryc. 5. Różne rodzaje fal elektromagnetycznych rejestrowanych podczas badań techniką WORP przy różnych offsetach

In Table 1, the electromagnetic properties assumed for further theoretical analysis are presented. The ranges of properties in the table result from the fact, that medium (i.e. flood levee) can be dry or water saturated (due to precipitation or melted snow).

The absolute values of reflection coefficients $|R_{TM}|$ and $|R_{TE}|$ were counted on the basis of the formulae (3, 4) and information from Table 1 and were presented in Fig. 6A; for counting, the following properties was assumed: $\epsilon_{r1} = 5$ ($Z_1 = 169 \Omega$) for dry mixture (sand+silt+slay) and $\epsilon_{r2} = 30$ ($Z_2 = 69 \Omega$) for water-saturated mixture. As it is seen in Fig. 6A, the increase of angle of incidence (resulting from the increase of the separation S) causes an increase of the value of $|R_{TE}|$, together with a simultaneous decrease the value of $|R_{TM}|$ until the Brewster's angle is achieved; above the Brewster's angle, both components increase. During the field tests, the influence of the discussed effects on the GPR recordings will be analysed. If the electromagnetic wave falls at the boundary at the angle of 90° (i.e. $\theta_i^{inc} = 0^\circ$), the reflection coefficient can be determined either from formulae (3, 4) or (1).

In Fig. 6B separations/offsets S counted on the basis of the formula (2) and information from Table 1 are

presented. Maximum height of the examined levee was 5 m, so for detection of loose zones in this levee, the antennae separations should change between 0.5 m and 5 m (for dry body of levee) or from 0.5 m to 2 m after precipitation.

3. THE TESTING WORP SURVEYS ON FLOOD LEVEE

The testing WORP measurements were carried out on the Vistula river flood levee in Cracow, Poland (Fig. 7A). In the publication [7] the results of the GPR surveys from this site were analysed to answer the question whether in the levee, the conditions for refraction GPR waves can be created. In the paper, the results obtained from the SORP and the WORP surveys, were presented and analysed.

Information obtained from the geotechnical sounding, made with the use of the dynamic probe light (DPL) called also the light dynamic penetrometer (LDP), revealed that material (Fig. 7B – mixture) in the examined levee is loose or partly semi-compacted (Fig. 7C).

The results of terrain measurements carried out in the investigation site in summer showed that no read-

Table 1. Material properties of media analysed in the paper [3]

Tabela 1. Parametry materiałowe ośrodków analizowanych w artykule [3]

Material	ϵ_r [-]	ν [m/ns]	μ_r [-]	σ [mS/m]
Sand (dry – water-saturated)	5 – 30	0.055 – 0.134	1	0.01 – 1
Silt (dry – water-saturated)	5 – 30	0.055 – 0.134	1	1 – 100
Clay (dry – water-saturated)	5 – 40	0.047 – 0.134	1	1 – 1000

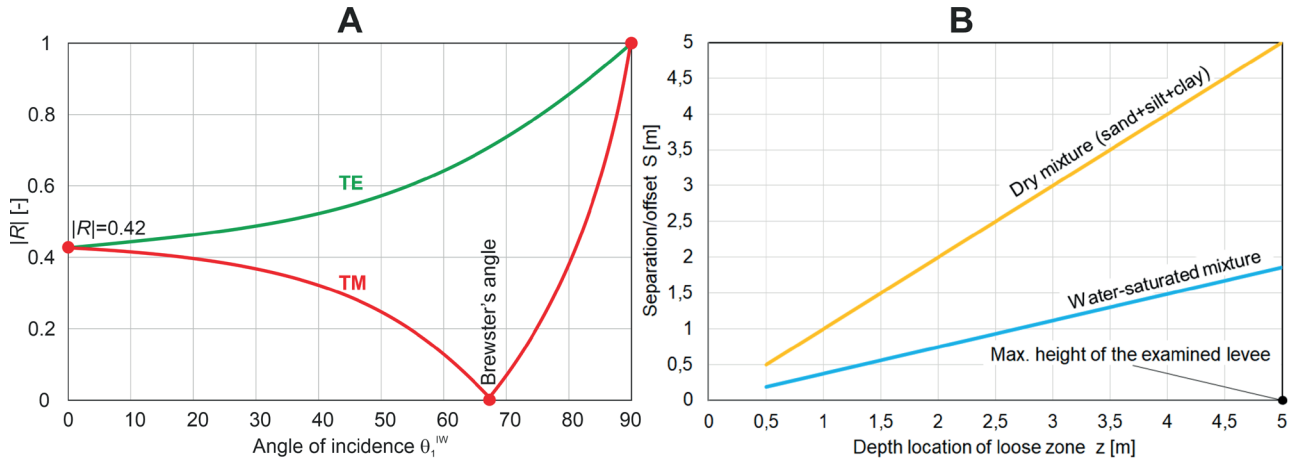


Fig. 6. A) The reflection coefficients for TE and TM components of the TEM wave for analysed media; B) The values of antennae separations S as a function of electromagnetic properties and loose zone location in the examined levee

Ryc. 6. A) Wartości współczynników odbicia dla składowych TE i TM fali typu TEM dla mediów analizowanych w artykule; B) Wartość odległości między antenami S jako funkcja parametrów materiałowych i położenia stref rozluźnień w badanym wale

able reflections were recorded in greater depths neither for short (Fig. 8A) nor for wide (Fig. 9C) offsets. Therefore, the terrain tests were conducted in autumn after precipitation, when sufficient max. antennae separation should be 2.0 m (Fig. 6B); the WORP surveys were carried out with values of S between 0.5–2.0 m with step of 0.5 m. After a rain, a near-surface, water-saturated zone as well as a deeper located dry zone were created in the examined levee; on the boundary of these zones, reflection coefficients $|R_{TM}|$ and $|R_{TE}|$ should be similar to those presented in Fig. 6A.

During the terrain surveys the following acquisition parameters for 200 MHz antennae (with mean resolution of 0.1 m and max. depth range of 10m) were assumed: traces were recorded with distance interval $\Delta x = 0.05$ m and stacking 32 times was applied to improve signal/noise ratio.

The measured GPR data were processed with the application of the following basic procedures: DC shift, dewow, phase correction, max. amplitude declipping, 1D median filter, Butterworth filter, gain function, background removal, 2D mean filter and static correction. For proper application of procedure of static correction, it is important to count the times t_{fa_DAW} of first arrivals of the DAW, depending of the antenna separations (Table 2). Detailed description of applied processing procedures may be found in the publications [3, 4, 8]. For processing and visualisation of GPR data, ReflexW software (www.sandmeier-geo.de)

was applied. All radargrams were presented in normalised scale.

For time-depth conversion of radargrams (Fig. 8, 9), mean velocity equals 0.10 m/ns was assumed on the basis of analyses presented in the publication [2]. In that publication, two zones with boundary at $z = 0.55$ m were defined after precipitation in the examined levee; the first was near-surface, water-saturated zone with velocity changing from 0.077 m/ns to 0.085 m/ns and the second was deeper located, dry zone with velocity between 0.11 m/ns and 0.12 m/ns; estimated velocities confirmed information from Table 1.

In radargrams no readable reflection were recorded below time 60 ns, therefore all recordings were cut at this time. In central part of selected radargrams

Table 2. The corrections of times t_{fa_DAW} of the first arrivals for the DAW for different antennae separations S

Tabela 2. Korekcje czasów t_{fa_DAW} pierwszych wstąpień fali DAW dla różnych odległości S pomiędzy antenami

Antennae frequency f [MHz]	Separations/offsets S [m]	Times of the first arrivals of the DAW t_{fa_DAW} [ns] for $v_{air} = 0.3$ m/ns
200	0.5	1.7
200	1.0	3.3
200	1.5	5.0
200	2.0	6.7

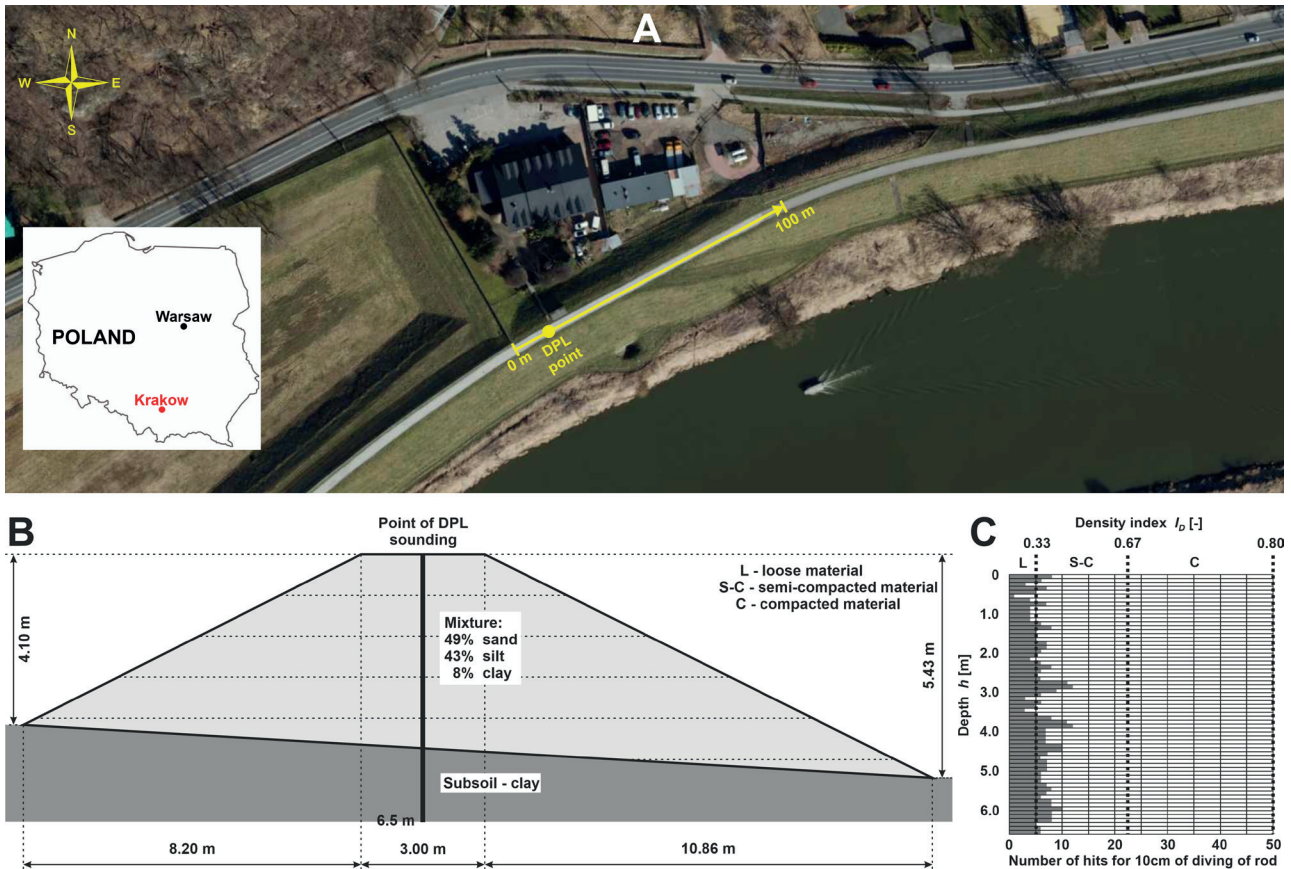


Fig. 7. A) The testing site of the SORP and the WORP surveys on the selected part of the Vistula river flood levee; B) Construction of the levee in the investigation site; C) The results of geotechnical DPL sounding

Ryc. 7. A) Miejsce testowania technik SORP i WORP na wybranym fragmencie wału wiślanego; B) Konstrukcja wału w miejscu badań; C) Wyniki sondowania dynamicznego DPL

(Fig. 8, 9) interference appeared and it was caused by any over-ground object (fence?) visible in Fig. 7A. In Figs. 8A, B and Fig. 9C this interference is invisible.

In Fig. 8B radargram recorded for antennae separation $S = 0.5$ m (i.e. for short-offset), was presented. In the figure, high-amplitude and linear reflections, beside direct waves, can be distinguished between $x = 13$ m and $x = 36$ m and from $x = 85$ m to $x = 94$ m; non-linear but high-amplitude reflections are also observed in distances $x = 38$ – 58 m. All these anomalies are located in the near-surface zone, to the approximated depth of c.a. 0.5 m. Taking into account the geotechnical information (Fig. 7C), the body of levee is more-less in the same stage of disintegration, so it was impossible to record reflections from any boundary. As it was mentioned before, after precipitation two zones were created and boundary between them became a reflector. Before precipitation (Fig. 8A) such reflector did not exist.

In order to check whether the WORP surveys could distinguish described above anomalies with better way, measurements were repeated along the same profile, with greater antennae separations, i.e.: $S = 1.0$ m (Fig. 8C), $S = 1.5$ m (Fig. 9A) and $S = 2.0$ m (Fig. 9B).

In Fig.8C, described previously anomalies are better visible, because they are separated from the direct waves, i.e. the DAW and the DGW. Interesting effect is, that anomaly in the first part of the profile is shorter now, but anomaly in the second part of the profile is much longer, then in Fig. 8B. In central part of the profile, anomalies have higher amplitudes than those, recorded in Fig. 8B. For situation presented in Fig. 8C, a value of S is equal 1.0 m, so angle of incidence is equal 45° (if reflector is located at $z = 0.5$ m); in such situation, increasing of reflection coefficient $|R_{TE}|$ with simultaneous decreasing of value of $|R_{TM}|$ are observed (Fig. 6A).

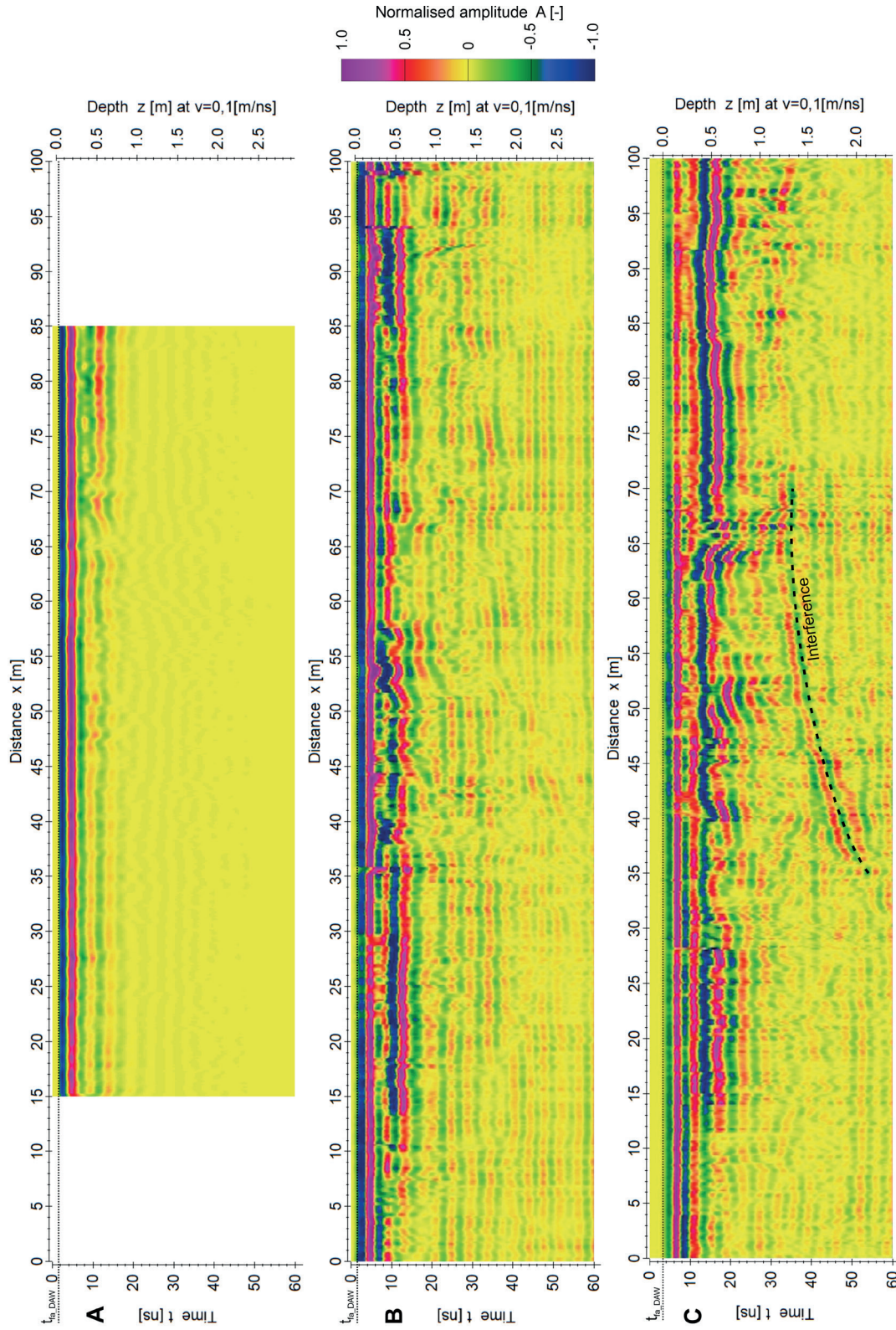


Fig. 8. Radargrams for antennae separations: A) $S = 0.5$ m (summer); B) $S = 0.5$ m (autumn); C) $S = 1.0$ m (autumn)
Ryc. 8. Radargramy dla odległości między antenami: A) $S = 0.5$ m (lato); B) $S = 0.5$ m (jesień); C) $S = 1.0$ m (jesień)

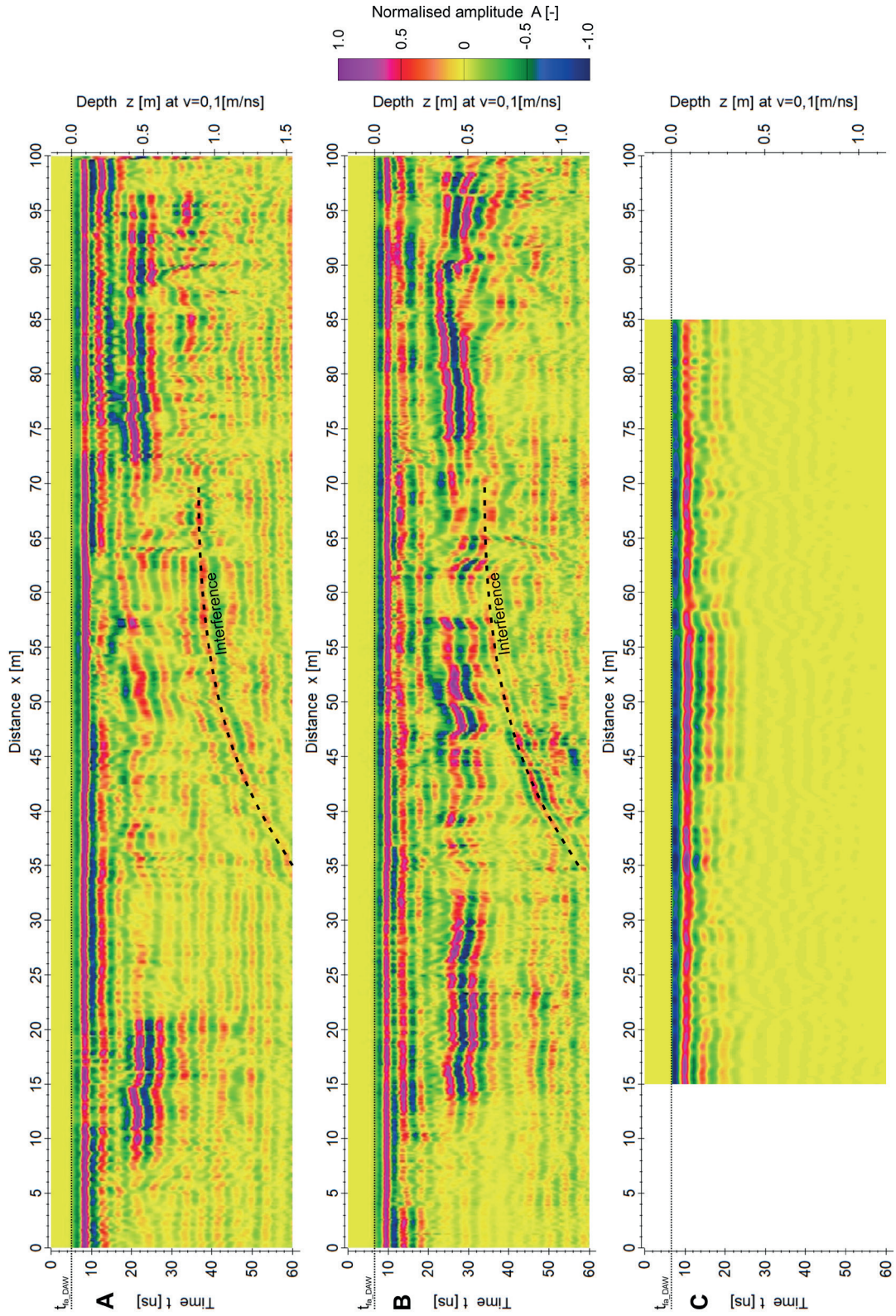


Fig. 9. Radargrams for antennae separations: A) $S = 1.5$ m (autumn); B) $S = 2.0$ m (autumn); C) $S = 2.0$ m (summer)
Ryc. 9. Radargramy dla odległości między antenami: A) $S = 1.5$ m (jesień); B) $S = 2.0$ m (jesień); C) $S = 2.0$ m (lato)

In Fig. 9A other interesting effects were recorded, i.e. left anomaly is similar in comparison with anomaly observed in Fig. 8C while right anomaly is similar to those visible in Fig. 8B; in central part of the profile, anomalies almost disappeared. In Fig. 9A radargram for separation $S = 1.5$ m is presented, so in consequence angle of incidence is equal 56° (with assumption that reflector is located at $z = 0.5$ m); in such situation angle of incidence approaches to the Brewster's angle and fast increasing of value of $|R_{TE}|$ with fast decreasing of value of $|R_{TM}|$ are observed (Fig. 6A).

In Fig. 9B all anomalies become a little longer than in Fig. 9A, and they appear again in the central part of the profile. This radargram was recorded for $S = 2.0$ m, so angle of incidence is equal 63° (if reflector is located at $z = 0.5$ m). The Brewster's angle is equal 68° (Fig. 6A) for example conditions assumed in the Section 2, i.e. was counted for dry and water-saturated mixtures. Perhaps, for antennae separation $S = 2.0$ m angle of incidence is greater than the Brewster's angle and than both reflection coefficients $|R_{TE}|$ and of $|R_{TM}|$ are increasing (Fig. 6A).

The radargram recorded for antennae separation 2.0 m before precipitation (Fig. 9C) is difficult for interpretation because in dry body of levee no conditions for electromagnetic wave reflections did not exist.

The analyses presented in publications [2, 7] deliver information that for separations 1.5 m (Fig. 9A) and 2.0 m (Fig. 9B), a refraction GPR wave appears in this site. The creation of the GPR refracted waves on the river levees for greater offsets was also confirmed and described in other works [9, 10, 11].

Comparing the results of terrain tests (Fig. 8, 9) it seems that the best visualisation of boundary between near-surface, water-saturated zone and deeper located dry zone was obtained in autumn, for antennae separation $S = 1.0$ m (Fig. 8C).

4. CONCLUSIONS

As it was shown in the paper, increasing the antennae separation results in better readability of anomalies recorded at small times/depths, because these anomalies are separated from the direct waves, i.e. from the direct air wave and the direct ground wave; in such a way, the effect of so-called "transmit pulse blanking" is reduced. The result of DPL sounding showed that the

body of examined levee can be treated as a uniformly disintegrated medium, so there should be no conditions for the reflection of electromagnetic waves from underground boundaries. This assumption was confirmed by the results of the GPR surveys carried out over a dry body of levee (in summer). The temporary reflectors appeared in the examined levee after precipitation (during the autumn surveys), because a two-layer medium was created, i.e. loose, near-surface, water-saturated zone and deeper located, better compacted, dry zone. The results of the field tests showed that in the selected part of the flood levee, a local reflectors was located at depth of c.a. 0.5 m, so the best result was achieved for antennae separation $S = 1.0$ m. The geotechnical sounding delivered information about loose material only in one point; it is very likely that along of 100 meters of the GPR profile, the porosity and water saturation in several parts of the examined levee will be different. This variability will influence to the local changes in both the shapes of the radiation patterns and the values of reflection coefficients, which will be affect the quality of recorded radargrams. Due to the all described variations, it is difficult to choice optimal offset before starting the measurements, therefore GPR surveys should be performed with various offsets to select the optimal antennae separation in the specific research site.

ACKNOWLEDGMENTS

The works were financed under the statutory activity of Department of Geoengineering and Water Management, Faculty of Environmental Engineering and Energy, Cracow University of Technology.

REFERENCES

1. Gołębowski, T. Flood levees and safety of towns. In proceeding of the 2nd conference on "Hydroengineering and Water Safety", Dobczyce, Poland, 24–25 June 2024 (in Polish).
2. Gołębowski, T. Application of the GPR method for detection and monitoring the objects with a stochastic distribution in a geological medium. AGH-UST Ed., Cracow, Poland, 2012; p. 254 (in Polish).
3. Annan, A.P. Ground Penetrating Radar – Applications, Principles and Procedures. Sensor and Software Inc., Canada, 1999; p. 278.

4. Annan, A.P. Ground Penetrating Radar – Workshop Notes. Sensor and Software Inc., Canada, 2001; pp. 192.
5. Arcone, S.A. Numerical studies of the radiation patterns of resistively loaded dipoles. *Journal of Applied Geophysics*, 1995; volume 33, pp. 39–52.
6. Gwarek, W., Morawski, T. Electromagnetic fields and waves. PWN-WNT Ed., Warsaw, Poland, 2024; p. 304 (in Polish).
7. Marcak, H., Gołębiowski, T., Tomecka-Suchoń, S. Analysis of the possibilities of using the GPR refraction waves to locate changes in the construction of flood levees. *Geology – quarterly of AGH-UST*, 2005; volume 31, issue 3–4, pp. 259–274 (in Polish).
8. Reflex W Manual. SandmeirGeo firm, Karlsruhe, Germany, 2024; pp. 729.
9. Gołębiowski, T. Changeable-offset GPR profiling for loose zones detection in levees. In proceedings of the 14th International Conference on “Near Surface 2008”, Cracow, Poland, 15–17 September 2008, pp. 1–5.
10. Dudkiewicz, M. The use of the GPR refractive waves to detect loose zones in the flood levees. Master Thesis, AGH-UST Cracow, Poland, 2007.
11. Parzymięso, M. The influence of the distance between the transmitter and the receiver antennae on the ability to identify parameters characterizing the geological structure. Master Thesis, AGH-UST Cracow, Poland, 2004.